

MIT Open Access Articles

Catalysis of Hydrogen–Deuterium Exchange Reactions by 4-Substituted Proline Derivatives

The MIT Faculty has made this article openly available. *Please share* how this access benefits you. Your story matters.

Citation: Myers, Eddie L. et al. "Catalysis of Hydrogen–Deuterium Exchange Reactions by 4-Substituted Proline Derivatives." *Journal of Organic Chemistry* 84, 3 (January 2019): 1247-1256
© 2019 American Chemical Society

As Published: <http://dx.doi.org/10.1021/acs.joc.8b02644>

Publisher: American Chemical Society (ACS)

Persistent URL: <https://hdl.handle.net/1721.1/123680>

Version: Author's final manuscript: final author's manuscript post peer review, without publisher's formatting or copy editing

Terms of Use: Article is made available in accordance with the publisher's policy and may be subject to US copyright law. Please refer to the publisher's site for terms of use.





Published in final edited form as:

J Org Chem. 2019 February 01; 84(3): 1247–1256. doi:10.1021/acs.joc.8b02644.

Catalysis of Hydrogen–Deuterium Exchange Reactions by 4-Substituted Proline Derivatives

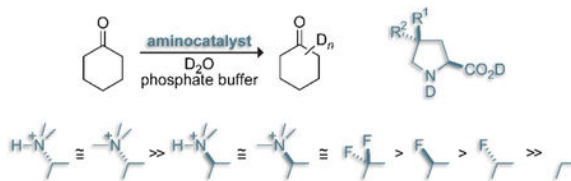
Eddie L. Myers^{*,†,‡}, Michael J. Palte[§], and Ronald T. Raines^{*,†,#,⊥}

[†]Department of Biochemistry, University of Wisconsin–Madison, 433 Babcock Drive, Madison, Wisconsin 53706, United States. [‡]School of Chemistry, NUI Galway, University Road, Galway, Ireland. [§]Medical Scientist/Molecular and Cellular Pharmacology Training Programs, University of Wisconsin–Madison, Madison, Wisconsin 53706, United States. [#]Department of Chemistry, University of Wisconsin–Madison, 1101 University Avenue, Madison, Wisconsin 53706, United States. [⊥]Department of Chemistry, Massachusetts Institute of Technology, 77 Massachusetts Avenue, Cambridge, Massachusetts 02139, United States.

Abstract

The identification and understanding of structure–activity relationships is vital for rational catalyst design. A kinetic study of the hydrogen–deuterium exchange reaction of cyclohexanone in aqueous solution, as catalyzed by proline derivatives, has revealed valuable structure–activity relationships. In phosphate-buffered solution, *cis*-4-fluoroproline is more active than the *trans* isomer, a distinction that appears to originate from a destabilizing interaction between the fluorine atom and phosphate anion during general acid catalyzed dehydration of the carbinolamine intermediate. *Trans*-4-ammoniumprolines are exceptionally active catalysts owing to favourable Coulombic interactions involving the ammonium group and the alkoxide moiety formed upon 1,2-addition of the proline derivative to the ketone. These results could be used for the optimisation of proline catalysts, especially in transformations where the formation of the putative iminium ion is rate-limiting.

Graphical Abstract



*Corresponding Authors R.T.R., rtraines@mit.edu; E.L.M., eddie.myers@nuigalway.ie.

ASSOCIATED CONTENT

Supporting Information

The Supporting Information is available free of charge on the ACS Publications website at DOI: [10.1021/acs.joc.xxxxxx](https://doi.org/10.1021/acs.joc.xxxxxx). NMR spectral data of catalysts, p*K*_a data, kinetic data and plots, (PDF).

Notes

The authors declare no competing financial interest.

INTRODUCTION

Transformations of saturated and unsaturated aldehydes and ketones in reactions catalyzed by small-molecule secondary amines, such as proline, are prevalent in organic synthesis.¹ Although initial reports on such aminocatalysis began as early as the late 19th century,² it was the appearance of reports from the research groups of Barbas, Lerner, List, and MacMillan in the late 1990s that began sustained interest in this area.³ Since the appearance of these early reports, aminocatalytic reactions have been shown to transform readily available substrates into diverse products with high levels of asymmetric induction, though turnover numbers remain low.⁴ The activity of small-molecule organocatalysts in water, in particular, is of interest because of potential benefits for the development of both environmentally friendly synthetic processes⁵ and tools for chemical biology.⁶ Furthermore, these investigations—and the exploration of the activity of enzymes in organic solvents—⁷ addresses the discontinuity between modern organocatalysis and native enzyme catalysis. The field of aminocatalysis is now maturing in that studies toward gaining greater mechanistic insight are taking center stage,⁸ a development that should facilitate catalyst design and could lead to commercially viable aminocatalytic processes.⁹

With an appreciation of the effect of 4-substituted prolines on the structure of protein,¹⁰ we decided to investigate the catalytic activity of 4-substituted prolines on a very simple transformation—the hydrogen–deuterium exchange reaction of ketones in aqueous solution, one of the earliest transformations to be investigated in the context of small-molecule aminocatalysis.¹¹ In a preliminary experiment (Scheme 1), we found that the catalytic activity of fluoroprolines on the hydrogen–deuterium exchange reaction of cyclohexanone in phosphate-buffered D₂O (pD 7.4) increased in the order *trans*-4-fluoroproline (**3**, p*K*_a 9.7) < *cis*-4-fluoroproline (**2**, p*K*_a 9.7) << 4,4-difluoroproline (**1**, p*K*_a 7.8).¹² The higher activity of *cis*-4-fluoroproline relative to the *trans* isomer (>2 fold) was intriguing and warranted further investigation. The relative levels of activity of 4-fluoroprolines has been investigated previously in the context of other organocatalytic reactions in organic solvents.¹³ For example, in a transannular aldol reaction, the use of the *trans* isomer gave higher yields and higher levels of asymmetric induction than that of the *cis* isomer.^{13a} The different levels of activity were proposed to originate from the strong preference of 4-fluoroproline derivatives to adopt a pyrrolidine ring pucker that places the fluoro group in a pseudo-axial orientation, a preference that has been attributed to the gauche effect.¹⁴ To determine the origin of the different levels of activity exhibited by the fluoroprolines we needed to fully understand the mechanism of the proline-catalyzed hydrogen–deuterium exchange reaction of cyclohexanone. In the 1960s and 1970s, Hine and co-workers found that the identity of the rate-limiting intermediate/transition state in amine-catalyzed isotope-exchange reactions of aldehydes and ketones depends on the nature of the catalyst, the substrate, and the reaction conditions.¹⁵ However, the exchange reaction has not been investigated for cyclohexanone and proline-based amines, leaving insufficient data to deduce the origin of the different levels of activity exhibited by the 4-fluoroproline derivatives. Herein, we show that the identity and orientation of substituents in 4-substituted proline derivatives have a substantial effect on the activity of these derivatives in the exchange reaction, and we explain the origin of these effects through the analysis of reaction kinetics.

Results and Discussion:

The rate of incorporation of deuterium into the α positions of cyclohexanone in phosphate-buffered D_2O at various pD values, as catalyzed by fluoroproline **1–3**, was measured by 1H NMR spectroscopy up until 10% conversion (Figure 1A). Spectra showed sets of resonances for the proline derivative and $[D_0]$ -cyclohexanone and its isotopologues; resonances associated with intermediates were not detected. The pD–rate profiles exhibit a maximum at pD values close to the pK_a value of the zwitterionic proline derivative. The exchange reaction was fastest at pD values close to 7 in the presence of 4,4-difluoroproline (**1**; pK_a 7.8), and *cis*-4-fluoroproline **2** (pK_a 9.7) is an approximately 2-fold more active catalyst than *trans*-4-fluoroproline **3** (pK_a 9.7). Catalysis by fluoroproline **1–3** is much more efficient than by unmodified proline: at ~pD 7.4, the rate of exchange as catalyzed by difluoroproline **1** is approximately 100 times that for proline. Above pD 10.0, as the pK_a value of proline is approached, the rate of exchange as catalyzed by proline increases rapidly; however, at these pD values, the background rate (buffer catalysis) also becomes significant (see Supporting Information). For each proline derivative, the order of the reaction with respect to each reaction component was determined using log/log plots of data obtained from the measurement of reaction rates at various concentrations of the reaction component, while keeping all other variables constant. The reactions exhibit component-specific orders of ~1 for cyclohexanone, the proline derivative, and phosphate at pD values close to maximum rate. The reaction order of phosphate buffer was determined by subtracting the low background rate associated with the aminocatalyst acting as both the putative covalent catalyst and as a donor/acceptor of a deuteron, thus the value of ~1 only includes transformations mediated through putative covalent catalysis by the proline derivative. Owing to the first order dependence of the rate of exchange on the buffer species, data for the reactions in imidazole-buffered D_2O were also obtained (Figure 1B). Interestingly, under these conditions, the *cis*- and *trans* 4-fluoroproline exhibited similar levels of activity, suggesting that the different levels of activity in phosphate buffer originate from an intimate interaction between a phosphate species and a fluoroproline-containing intermediate.

Substrate isotope effects were determined by measuring the rates of exchange of the α hydrogen atoms of $[D_0]$ -cyclohexanone and the α deuterium atoms of $[D_4]$ -cyclohexanone as catalyzed by **1** in 1:1 mixtures of phosphate-buffered D_2O and H_2O (150 mm, $I = 0.9$). The use of a common solvent (H_2O/D_2O , 1:1) allows the substrate isotope effect to be disentangled from solvent isotope effects. GC-MS analysis of aliquots taken from reaction mixtures at pH-meter values of 6 and 8 with consideration of the fractionation factors (ϕ , $[DA]/[HA]$ in D_2O/H_2O 1:1) of the major deuteron- and proton-donating species at these pH-meter values ($D_2PO_4^-/H_2PO_4^-$, $\phi = 1.03$; DPO_4^{2-}/HPO_4^{2-} , $\phi = 0.91$),¹⁶ gave k_H/k_D values of ~1 (Figure 1D, Table 1). The solvent isotope effect for the exchange reaction catalyzed by proline **1** was determined by comparing rates of reactions carried out in D_2O with those in D_2O/H_2O (1:1) at various pH-meter values (Figure 1C). Considering that approximately half of the exchange events in D_2O/H_2O (1:1) are unobservable, that is, a hydrogen atom is exchanged for another hydrogen atom (as supported by substrate isotope effects), the maximum rate of exchange in D_2O was found to be ~5-fold higher than that in D_2O/H_2O (1:1), thus pointing toward a remarkably large inverse solvent isotope effect.

The absence of a primary isotope effect is consistent with the rate-determining step occurring prior to the putative interconversion of iminium **D** and enamine **E** (Scheme 1). The absence of a significant secondary isotope effect, which, for example, can range from 0.8–1.2 for addition reactions of [D₀]- and [D₆]-acetone,¹⁷ is consistent with one of two scenarios: i) proline **1** undergoes rate-determining addition to cyclohexanone with an early transition state; ii) the putative carbinolamine **C**, which is in equilibrium with starting material, undergoes rate-determining dehydration, the associated kinetic secondary isotope effect completely offsetting the preceding equilibrium secondary isotope effect. Additionally, analysis of the change in the relative amounts of [D₀]-cyclohexanone and its isotopologues over the course of the reaction show that only one deuterium atom is incorporated at a time, that is, [D₂]-cyclohexanone is formed via [D₁]-cyclohexanone (see mass spectrometry data in the Supporting Information). This observation suggests that the distal and proximal axially orientated α hydrogen atoms with respect to the carboxylate group of the putative iminium ion undergo abstraction as protons with very different rates and that [D₁]-iminium ion ([D₁]-**D1**, Scheme 2) is converted into [D₁]-cyclohexanone faster than any process that would lead to its conversion into a stereoisotopomer, for example, conversion into the [D₁]-iminium ion where the incorporated deuterium atom would lie in an equatorial position ([D₁]-**D2**, Scheme 2). Previously obtained crystal structures of proline-based enamines derived from ketones suggest that the more acidic hydrogen atom is that whose abstraction leads directly to the enamine intermediate in which the carboxylate group is anti to the C=C bond (Scheme 2, inset).¹⁸ In an investigation reported by Hine and co-workers on the exchange reaction of [D₆]-acetone in aqueous buffer catalyzed by bifunctional primary–tertiary diamines, [D₃]- and [D₄]-acetone were formed at the very beginning of the reaction, with [D₅]-acetone not being detected.¹⁹ The pendant tertiary amine base and the ability of the iminium ion derivative of acetone to undergo rapid rotation about the C–C bonds contributed to this extremely efficient rate of exchange.

The above data are consistent with the following mechanism (see Scheme 1): a) Addition of the proline derivative to cyclohexanone to give the carbinoxyammonium **A**, which requires an acid (H₂PO₄⁻/HPO₄²⁻) for conversion into carbinolammonium **B**; owing to steric considerations, addition is likely to proceed through attack of the proline face opposite the carboxylate group. b) Carbinolammonium **B** can then either be converted back into starting material involving base-mediated deprotonation of the OH group, or, via its conjugate base, carbinolamine **C**, undergo rate-determining acid-mediated dehydration to iminium **D**. Similarly, Hine and co-workers have shown that acid-mediated dehydration of carbinolamines derived from aldehydes and primary amines to give the corresponding iminium ion is rate determining in acidic to neutral aqueous solution.²⁰ c) In D₂O, the corresponding OD group of carbinolammonium **B** undergoes dedeuteriation at a slower rate owing to a primary isotope effect, thus leading to greater partitioning of carbinolamine **C** into iminium **D** and a faster rate of exchange, a situation that manifests as a large inverse solvent isotope effect. Large inverse solvent isotope effects are rare but are observed in E1cB reactions, where rate-determining expulsion of the β-positioned leaving group competes with protonation of the intermediate carbanion.²¹ d) In the more stable chair conformer, the axial hydrogen atom distal and *anti* to the proline carboxylate moiety of iminium **D** (Scheme 2) undergoes deprotonation to give enamine **E**, which is ultimately transformed back into

ketone via intermediates **D**, **C**, **B**, and **A** at a rate faster than any other process that would lead to the exchange of any of the remaining three hydrogen atoms.

The experimentally supported reaction coordinate suggests that the lower rate of exchange of cyclohexanone in phosphate-buffered D₂O in the presence of *trans*-4-fluoroproline **3** might be due to differences in the transition state linking carbinolamine **C** and iminium **D**. Specifically, dehydration of carbinolamine **C** derived from fluoroproline **3** may be inhibited by a destabilizing Coulombic interaction between the electronegative fluorine atom, which, owing to the gauche effect, will be moving towards an axial position, and the phosphate species, which as it delivers a proton, will be becoming more anionic (Scheme 3A). Presumably, in imidazole buffer, the corresponding proton transfer from the cationic imidazolium ion does not present a differentiating impediment. A similar destabilizing interaction in the phosphate-mediated protonation of carbinoxyammonium **A** (Scheme 3B) is likely to be less important owing to the early transition state in this transformation. Note, it is reasonable to assume that this transformation (protonation of the carbinoxyammonium **A**) has an early transition state because the reverse reaction (deprotonation of the carbonolammonium **B**) has been proposed to contribute to the large inverse solvent isotope effect and thus would be deemed to proceed through a late transition state.

To further explore the effect of the identity and relative configuration of substituents at the 4-position on the catalytic activity of proline derivatives, we prepared the *cis* and *trans* isomers of both 4-dimethylammonium and 4-trimethylammonium proline (Figure 2) from commercially available *N*-*tert*-butoxycarbonyl (*N*-Boc)-protected 4-hydroxyprolines.

The *cis* isomers, **4** and **6**, were prepared from *trans* *N*-Boc-hydroxyproline methyl ester (Scheme 4). Activation of the C4 hydroxy group as the mesylate followed by invertive displacement with azide ion gave the *cis* 4-azidoproline derivative.²² Hydrogenative reduction of the azide followed by reductive alkylation in the presence of formalin gave protected *cis* 4-dimethylaminoproline **8**, which was treated sequentially under basic and acidic conditions to effect saponification and removal of the Boc group to give *cis* 4-dimethylaminoproline dihydrochloride salt (**4**). Alternatively, *N*-methylation of dimethylaminoproline derivative **8** gave the trimethylammonium iodide derivative, which, owing to light sensitivity conferred by the iodide ion on this compound and subsequent derivatives, was treated with ion-exchange resin so that iodide could be replaced by chloride. Saponification and removal of the Boc group gave *cis* 4-trimethylammoniumproline salt **6**. The *trans* isomers, **5** and **7**, were prepared from *cis* *N*-Boc-hydroxyproline by using an identical protocol (not depicted, see Experimental Section).

pD profiles show that the *trans* diastereomers of dimethyl-ammonium proline **5** (p*K*_a 7.4, 10.3) and trimethylammonium proline **7** (p*K*_a 7.4), are exceptionally active catalysts with maximum rates ~10- and 5-fold higher than those for the reactions catalyzed by the corresponding *cis* diastereomers, **4** and **6**, which were of the level observed for fluoroproline **1** (Figure 3A,B). Similar to the exchange reaction catalyzed by the fluoroproline, reactions catalyzed by the aminoproline exhibited component-specific orders of ~1 for cyclohexanone, the proline derivative, and phosphate/imidazole at pD values close to maximum rate. Further investigation of reactions catalyzed by ammoniumproline **7** showed

no substrate isotope effect and a large solvent isotope effect (rate in D₂O~9-fold greater than that in D₂O/H₂O, 1:1; Figure 3D). Notably, although most pD–rate profiles exhibit a pronounced maximum that span a narrow pD range, the pD–rate profile of **6** elicits a sharp rise in rate to a maximum value as the pD approaches that corresponding to the p*K*_a of **6** (7.4) and maintains this value in the pD range 7.9–10.5, before the rate falls gradually.

We believe that the origin of the exceptional levels of activity of *trans* 4-aminoprolines **5** and **7** is that nucleophilic attack of the proline derivative on the ketone would place the resulting carboxy group in close proximity to the ammonium group at the 4-position of the pyrrolidine ring (Scheme 5). The stabilizing Coulombic interaction between these two groups should engender a relatively high concentration of carboxyammonium **A** and thus lead to a relatively high rate of exchange. Electrostatic interactions, of the type proposed above, are known to promote reactions involving the addition of nucleophiles to carbonyl compounds. For example, the nonenzymatic hydrolysis of acetylcholine (2-trimethylammoniummethyl acetate) in basic aqueous solution is significantly faster than that of ethyl acetate, and there is strong evidence that suggest that an electrostatic interaction between the oxyanion group and the trimethylammonium group in the putative tetrahedral intermediate is the origin of this rate enhancement.²³ Aminoproline **5**, which shows the highest level of activity, albeit only within a narrow pD range close to its p*K*_a value, would be expected to generate a higher concentration of carboxyammonium **A** relative to that of **7** because of lower levels of steric hindrance. There is no evidence to suggest that the presumed ability of the dimethylammonium group to transfer a proton to the carboxy group contributes to a higher rate of the exchange reaction catalyzed by **5**; presumably, the reverse proton transfer (from oxygen to nitrogen) is so fast that an external acid is still required. The rate-determining step for the reactions catalyzed by prolines **5** and **7** appears to be the dehydration of carbinolamine **C**. However, the shape of the pD profiles of the *cis*-dimethyl- and *cis*-trimethylammonium prolines, **4** and **6**, is more consistent with the rate-determining step being the acid-catalyzed addition of the proline derivative to cyclohexanone. The large inverse solvent isotope effect measured for the reactions catalyzed by prolines **1** and **7** suggests that for the formation of the carbinolamine in these reactions, the transfer of the proton from the acid to the alkoxide occurs quite late in the transition, thus making this step insensitive to the p*K*_a of the acid and only dependent on the total amount of acid available. The observation that the rate associated with *cis* 4-aminoprolines, **4** and **6**, remains essentially constant over a wide pD range but drops significantly at pD values higher than 10.5 (phosphate buffer) and 7 (imidazole buffer), at which point the total concentration of acid will start to decrease, is consistent with this hypothesis.

The relatively sharp maxima of the pD profiles of catalysis by fluoroproline **1** (Figure 1A) and aminoprolines **5** and **7** (Figure 3A, B) deserves further comment. For example, the exchange reaction catalyzed by fluoroproline **1** reaches a maximum rate at pD 7.4, close to the p*K*_a value of fluoroproline **1** (7.8), but falls rapidly as the pD value increases further. Although the amount of fluoroproline available for covalent catalysis should continue to increase for a region beyond pD 7.4 (at pD 7.8, 50% of the catalyst will still be in the ammonium form), the overall strength of the available acids will tend to decrease and the overall strength of the available bases will tend to increase (as D₂PO₄[−] is being partitioned

into DPO_4^{2-} ; and **1.D** into the free amine **1**—the catalyst also acts as donor and acceptor of deuterons). Therefore, the overall rate constant associated with the base-catalysed conversion of carbinolammonium **B** into **A** will increase and that associated with the acid-catalysed conversion of carbinolamine **C** into iminium ion **D** will decrease, thus causing the overall rate of exchange to fall. For difluoroproline catalyst **1**, the rates of exchange as a function of phosphate concentration have been determined at pD 6.5 and pD 8.5 ($I = 0.9$). From the intercept of the concentration-versus-rate plots, the minor contribution to the overall rate associated with the protonated form of the catalyst acting as an acid (rather than phosphate buffer) can be ascertained. If these contributions are subtracted, the relative contribution of $[\text{D}_2\text{PO}_4^-]$ and $[\text{DPO}_4^-]$ can be determined, with the assumption that the contribution of catalysis by $[\text{D}_3\text{O}^+]$ is negligible. Using the Henderson-Hasselbalch equation and the $\text{p}K_a$ values of aminocatalyst (7.8) and D_2PO_4^- (6.7), a value of ~ 33 is estimated for the relative contribution to the overall rate of catalysis by the mono- and dianionic forms of the buffer, $k(\text{D}_2\text{PO}_4^-)/k(\text{DPO}_4^-)$. Using these values, the maximum of a simulated pD-rate profile for **1** (pD 7.4) agrees with the value experimentally determined (see Supporting Information).

CONCLUSIONS

Our findings provide fundamental insight on the design of efficient aminocatalytic systems for transformations in water. Despite the highly stabilizing effect of water as solvent, inter- and intramolecular electrostatic interactions involving charged and electron-rich atoms derived from substrate, catalyst, and buffer can have a dramatic influence on catalytic activity. We believe that *cis*- and *trans*-4-trimethyl ammoniumproline are especially promising in that context.

EXPERIMENTAL METHODS

General Methods.

Procedures were performed at room temperature (~ 23 °C) unless indicated otherwise. Reactions were monitored by thin-layer chromatography using Whatman® aluminum-backed silica gel TLC plates with visualization by UV light or ninhydrin staining. Compounds were purified by flash chromatography on silica gel, which had a mesh of 230–400 (ASTM) and a pore size of 60 Å. The removal of solvents and other volatile materials “under reduced pressure” refers to the use of a rotary evaporator at water-aspirator pressure (< 20 torr) and a water bath of < 40 °C. Compounds “dried under vacuum” refers to the placement of the material on a manifold connected to an oil-based pump capable of maintaining pressures of < 0.1 Torr. Fluoroprolines and protected forms of *cis*- and *trans*-hydroxyprolines (for the preparation of aminoprolines) are commercially available.

Instrumentation.

NMR spectra were acquired at ambient temperature with a Bruker DMX-400 Avance spectrometer (^1H , 400.1 MHz; ^{13}C , 100.6 MHz) at the National Magnetic-Resonance Facility at Madison (NMRFAM). The detection of ^{13}C nuclei was proton decoupled. ^1H NMR spectra were referenced to TMS or to the residual solvent peak. ^{13}C NMR spectra

were referenced to the residual solvent peak. Mass spectrometry was performed with a Waters Micromass LCT®: electrospray ionization, time of flight; GCMS was performed with a Shimadzu GCMS-QP2010S (gas chromatography, electron impact, single quadrupole) in the Mass Spectrometry Facility in the Department of Chemistry at the University of Wisconsin–Madison.

Synthesis of Aminoproline Derivatives.

1-tert-Butyl-2-methyl (2S,4S)-4-(dimethylamino)pyrrolidine-1,2-dicarboxylate (8).—A stream of Ar(g) was continuously passed through a 250-mL 3-neck flask equipped with stirring bar. 10 % Pd/C (0.4 g) was added followed by MeOH (50 mL). A solution of 1-*tert*-butyl-2-methyl-(2*S*,4*S*)-4-azidopyrrolidine-1,2-dicarboxylate (3.15 g, 11.66 mmol)²² in MeOH (50 mL) was added, and the suspension was cooled to 0 °C. The flask was evacuated and placed under a balloon of H₂(g). The stirred suspension was warmed to room temperature overnight. The balloon was removed, and the suspension was placed under Ar(g). Formalin (2 mL) was added, and the flask was again evacuated and placed under a balloon of H₂(g). The resulting mixture was stirred overnight at room temperature. The balloon was removed, and the suspension was carefully filtered through Celite®; the residue was washed with MeOH (100 mL). The filtrate was evaporated, and the resulting oil was taken up in CH₂Cl₂. The solution was washed with sat. aq. NaHCO₃ (2 × 50 mL), dried over Na₂SO₄(s), and evaporated. The residue was purified by silica gel column chromatography (eluent: 1–2% MeOH/CH₂Cl₂). The resulting pale-yellow oil was placed under house vacuum overnight (2.1 g, 7.72 mmol, 66% yield). ¹H NMR (400 MHz, CDCl₃, mixture of rotamers 2:1; designated major (ma.) and minor (mi.) where possible): δ = 1.40 (ma.) and 1.46 (mi.) (9H, s), 1.72–1.86 (1H, m), 2.17–2.24 (6H, m), 2.37–2.52 (1H, m), 2.54–2.68 (1H, m), 3.13–3.24 (1H, m), 3.63–3.88 (4H, m), 4.19–4.32 (1H, m). ¹³C NMR{1H} (100.6 MHz, CDCl₃, mixture of rotamers; designated major (ma.) and minor (mi.) where possible): δ = 28.2 (ma.), 28.3 (mi.), 34.4 (mi.), 36.1 (ma.), 44.2 (mi.), 44.3 (ma.), 50.5 (ma.), 50.7 (mi.), 51.9 (ma.), 52.1 (mi.), 58.1 (mi.), 58.6 (ma.), 63.8 (ma.), 64.4 (mi.), 80.1 (ma. and mi.), 153.5 (ma.), 154.1 (mi.), 172.8 (mi.), 173.1 (ma.). HRMS (ESI-TOF) *m/z*: [M + H]⁺ Calcd for C₁₃H₂₅N₂O₄ 273.1809; Found 273.1810.

1-tert-Butyl-2-methyl-(2S,4S)-4-(trimethylammonium)pyrrolidine-1,2-dicarboxylate Chloride (9).—1-*tert*-Butyl-2-methyl (2*S*,4*S*)-4-(dimethylamino)pyrrolidine-1,2-dicarboxylate (**8**, 0.94 g, 3.45 mmol) was dissolved in CH₂Cl₂ (10 mL). MeI (1.07 mL, 17.26 mmol) was added, and the resulting solution was allowed to stir at room temperature overnight. The volatiles were then removed by rotary evaporation to give a foamy white solid. The solid was dissolved in MeOH (5 mL) anionic ion exchange resin (Amberlite IRA410–chloride form) was added (~15 equiv). The resulting suspension was allowed to stir for 10 min and was then filtered; the resin was washed with a portion of MeOH (5 mL). The combined filtrates were evaporated to give a white solid (0.98 g, 3.04 mmol, 88% yield). ¹H NMR (400 MHz, CDCl₃, mixture of rotamers, broad signals): δ = 1.40–1.46 (9H, m), 2.26–2.37 (1H, m), 2.86–2.96 (1H, m), 3.44–3.50 (9H, m), 3.57–3.65 (1H, m), 3.71–3.75 (3H, m), 3.98–4.06 (1H, m), 4.32–4.40 (1H, m), 4.76–4.90 (1H, m). ¹³C NMR{1H} (100.6 MHz, CDCl₃, broad signals): δ = 28.1, 30.3, 45.3, 52.8, 53.5, 57.1,

70.0, 81.5, 152.9, 171.6. HRMS (ESI-TOF) m/z : $[M]^+$ Calcd for $C_{14}H_{27}N_2O_4$ 287.1966; Found 287.1974.

1-tert-Butyl-2-methyl-(2S,4R)-4-(dimethylamino)pyrrolidine-1,2-dicarboxylate (10).—A stream of Ar(g) was continuously passed through a 250-mL 3-neck flask equipped with stirring bar. 10% Pd/C (0.4 g) was added followed by MeOH (50 mL). A solution of 1-*tert*-butyl-2-methyl-(2*S*,4*R*)-4-azidopyrrolidine-1,2-dicarboxylate (3.22 g, 11.92 mmol)^{22,24} in MeOH (50 mL) was added, and the suspension was cooled to 0 °C. The flask was evacuated and placed under a balloon of H₂(g). The stirred suspension was warmed to room temperature overnight. The balloon was removed, and the suspension was placed under Ar(g). Formalin (2 mL) was added, and the flask was again evacuated and placed under a balloon of H₂(g). The resulting mixture was stirred overnight at room temperature. The balloon was removed, and the suspension was carefully filtered through Celite®; the residue was washed with MeOH (100 mL). The filtrate was evaporated, and the resulting oil was taken up in CH₂Cl₂. The solution was washed with sat. aq. NaHCO₃ (2 × 50 mL), dried over Na₂SO₄(s), and evaporated. The residue was purified by silica gel column chromatography (eluent: 1–2% MeOH/CH₂Cl₂). The resulting pale-yellow waxy solid was placed under house vacuum overnight (2.45 g, 9.00 mmol, 76% yield). ¹H NMR (400 MHz, CDCl₃, mixture of rotamers 60:40; designated major (ma.) and minor (mi.) where possible): δ = 1.38 (ma.) and 1.44 (mi.) (9H, s), 2.00–2.23 (8H, m), 2.73–2.88 (1H, m), 3.08–3.22 (1H, m), 3.65–3.83 (4H, m), 4.30 (ma.) and 4.39 (mi.) (1H, m). ¹³C NMR{1H} (100.6 MHz, CDCl₃, mixture of rotamers; designated major (ma.) and minor (mi.) where possible): δ = 28.2 (ma.), 28.3 (mi.), 34.0 (mi.), 35.0 (ma.), 44.1 (ma. and mi.), 50.3 (ma.), 50.6 (mi.), 52.0 (ma.), 52.1 (mi.), 58.2 (mi.), 58.7 (ma.), 62.8 (ma.), 63.6 (mi.), 80.0 (ma. and mi.), 153.5 (ma.), 154.2 (mi.), 173.1 (mi.), 173.4 (ma.). HRMS (ESI-TOF) m/z : $[M + H]^+$ Calcd for $C_{13}H_{25}N_2O_4$ 273.1809; Found 273.1805.

1-tert-Butyl-2-methyl-(2S,4R)-4-(trimethylammonium)pyrrolidine-1,2-dicarboxylate chloride (11).—1-*tert*-Butyl-2-methyl (2*S*,4*R*)-4-(dimethylamino)pyrrolidine-1,2-dicarboxylate (**10**, 0.93 g, 3.41 mmol) was dissolved in CH₂Cl₂ (10 mL). MeI (1.07 mL, 17.26 mmol) was added, and the resulting solution was allowed to stir at room temperature overnight. The volatiles were then removed by rotary evaporation to give a foamy white solid. The solid was dissolved in MeOH (5 mL), and anionic ion exchange resin (Amberlite IRA410–chloride form) was added (~15 equiv). The resulting suspension was allowed to stir for 10 min and was then filtered; the resin was washed with a portion of MeOH (5 mL). The combined filtrates were evaporated to give a white solid (1.03 g, 3.2 mmol, 94% yield). ¹H NMR (400 MHz, CDCl₃, mixture of rotamers 2:1; designated major (ma.) and minor (mi.) where possible): δ = 1.35 (ma.) and 1.43 (mi.) (9H, m), 2.47–2.58 (1H, m), 2.82–3.02 (1H, m), 3.45–3.53 (9H, m), 3.64–3.78 (4H, m), 3.87–3.96 (1H, m), 4.46–4.56 (1H, m), 4.57–4.76 (1H, m). ¹³C NMR{1H} (100.6 MHz, CDCl₃, mixture of rotamers designated major (ma.) and minor (mi.) where possible): δ = 28.1 (ma.), 28.3 (mi.), 29.8 (mi.), 30.7 (ma.), 45.4 (ma. and mi.), 52.7 (ma. and mi.), 53.0 (ma.), 53.5 (mi.), 57.6 (mi.), 57.8 (ma.), 71.2 (ma.), 72.0 (mi.), 81.4 (ma.), 81.7 (mi.), 153.0 (ma.), 153.4 (mi.), 171.7 (mi.), 171.8 (ma.). HRMS (ESI-TOF) m/z : $[M]^+$ Calcd for $C_{14}H_{27}N_2O_4$ 287.1966; Found 287.1974.

(2S,4S)-4-(dimethylamino)pyrrolidine-2-carboxylic Acid Dihydrochloride (4·2HCl).—1-*tert*-Butyl-2-methyl-(2*S*,4*S*)-4-(dimethylamino)pyrrolidine-1,2-dicarboxylate (**8**, 1.17 g, 4.30 mmol) was dissolved in 1,4-dioxane (10 mL). 1 M NaOH in H₂O (4.5 mL, 4.5 mmol) was added, and the resulting solution was allowed to stir at room temperature overnight. The volatiles were then removed by rotary evaporation. The solid was redissolved in 4 M HCl in 1,4-dioxane (10 equiv, 10.8 mL), and the resulting solution was allowed to stir for 30 min at room temperature. The volatiles were removed by rotary evaporation to leave a white solid (1.0 g, 4.3 mmol, quantitative). NMR analysis showed that the compound was pure. ¹H NMR (400 MHz, D₂O): δ = 2.28 (1H, ddd, *J* = 12.5, 10.7, 9.5 Hz), 2.84 (3H, s), 2.85 (3H, s), 2.92 (1H, ddd, *J* = 12.5, 7.6, 7.6 Hz), 3.55 (1H, dd, *J* = 12.9, 8.9 Hz), 3.86 (1H, dd, *J* = 12.9, 8.5 Hz), 4.14 (1H, dddd, *J* = 9.5, 8.9, 8.5, 7.6 Hz), 4.50 (1H, dd, *J* = 10.7, 7.6 Hz). ¹³C NMR{1H} (100.6 MHz, D₂O): δ = 29.5, 42.2, 42.6, 45.0, 58.3, 62.9, 169.2. HRMS (ESI-TOF) *m/z*: [M+1]⁺ Calcd for C₇H₁₅N₂O₂ 159.1123; Found 159.1129.

(2S,4R)-4-(Dimethylamino)pyrrolidine-2-carboxylic acid dihydrochloride (5·2HCl).—1-*tert*-Butyl-2-methyl-(2*S*,4*R*)-4-(dimethylamino)pyrrolidine-1,2-dicarboxylate (**10**, 0.92 g, 3.39 mmol) was dissolved in 1,4-dioxane (10 mL). 1 M NaOH in H₂O (3.56 mL, 3.56 mmol) was added, and the resulting solution was allowed to stir at room temperature overnight. The volatiles were then removed by rotary evaporation. The solid was redissolved in 4 M HCl in 1,4-dioxane (10 equiv, 8.5 mL), and the resulting solution was allowed to stir for 30 min at room temperature. The volatiles were removed by rotary evaporation to leave a white solid (0.79 g, 3.39 mmol, quantitative). NMR analysis showed that the compound was pure. ¹H NMR (400 MHz, D₂O): δ = 2.61 (1H, ddd, *J* = ~15, 8.8, 8.8 Hz), 2.78 (1H, ddd, *J* = ~15, 7.5, 7 Hz), 2.90 (6H, br. s), 3.60 (1H, dd, *J* = 12.6, 8.5 Hz), 3.98 (1H, dd, *J* = 12.6, 8.2 Hz), 4.16 (1H, dddd, *J* = 8.8, 8.5, 8.2, 7.5 Hz), ~4.65 (1H, multiplet obscured by residual solvent). ¹³C NMR{1H} (100.6 MHz, D₂O): δ = 29.6, 42.2, 42.4, 45.4, 58.8, 62.6, 170.0. HRMS (ESI-TOF) *m/z*: [M+Na]⁺ Calcd for C₇H₁₄N₂NaO₂ 181.0953; Found 181.0947.

(2S,4S)-4-(Trimethylammonium)pyrrolidine-2-carboxylic Acid Chloride Hydrochloride (6·2HCl).—1-*tert*-Butyl-2-methyl-(2*S*,4*S*)-4-(trimethylammonium)pyrrolidine-1,2-dicarboxylate chloride (**9**, 0.98 g, 3.04 mmol) was dissolved in 1,4-dioxane (10 mL). 1 M NaOH in H₂O (3.2 mL, 3.19 mmol) was added, and the resulting solution was allowed to stir at room temperature overnight. The volatiles were then removed by rotary evaporation. The solid was redissolved in 4 M HCl in 1,4-dioxane (10 equiv, 7.6 mL), and the resulting solution was allowed to stir for 30 min at room temperature. The volatiles were removed by rotary evaporation to leave a white solid (0.75 g, 3.04 mmol, quantitative). NMR analysis showed that the compound was pure. ¹H NMR (400 MHz, D₂O, pD = 5.1, 150 mM phosphate, *I* = 0.9): δ = 2.37 (1H, m), 2.87 (1H, m), 3.17 (9H, s), 3.74 (1H, m), 3.88 (1H, m), 4.27 (1H, m), 4.48 (1H, m). ¹³C NMR{1H} (100.6 MHz, D₂O, pD = 5.1, 150 mM phosphate, *I* = 1.5): δ = 28.5, 43.0, 51.9, 59.9, 70.8, 171.6. HRMS (ESI-TOF) *m/z*: [M]⁺ Calcd for C₈H₁₇N₂O₂ 173.1285; Found 173.1283.

(2S,4R)-4-(trimethylammonium)pyrrolidine-2-carboxylic Acid Chloride Hydrochloride (7·2HCl).—1-*tert*-Butyl-2-methyl-(2*S*,4*R*)-4-

(trimethylammonium)pyrrolidine-1,2-dicarboxylate chloride (**11**, 1.03 g, 3.20 mmol) was dissolved in 1,4-dioxane (10 mL). 1 M NaOH in H₂O (3.4 mL, 3.40 mmol) was added, and the resulting solution was allowed to stir at room temperature overnight. The volatiles were then removed by rotary evaporation. The solid was redissolved in 4 M HCl in 1,4-dioxane (10 equiv, 8.0 mL), and the resulting solution was allowed to stir for 30 min at room temperature. The volatiles were removed by rotary evaporation to leave a white solid (0.79 g, 3.20 mmol, quantitative). NMR analysis showed that the compound was pure. ¹H NMR (400 MHz, D₂O): δ = 2.72–2.80 (2H, m), 3.13 (9H, s), 3.75 (1H, dd, J = 13.2, 8.4 Hz), 3.97 (1H, dd, J = 13.2, 8.7 Hz), 4.45 (1H, dddd, J = 8.7, 8.4, ~8, ~8 Hz), ~4.70 (1H, multiplet obscured by residual solvent). ¹³C NMR {1H} (100.6 MHz, D₂O): δ = 27.8, 43.7, 52.0, 58.5, 69.9, 169.4. HRMS (ESI-TOF) m/z : [M]⁺ Calcd for C₈H₁₇N₂O₂ 173.1285; Found 173.1281.

Determination of pK_a Values.—The logarithmic acidity constants (pK_a values) of the proline derivatives used in this study in environments that are relevant and normal to the reaction under investigation (D₂O, 150 mM phosphate, I = 0.9) were determined using ¹H NMR spectroscopy. Acidic and alkaline 30 mM D₂O solutions of the proline derivative under investigation were prepared by adding the required amount of catalyst (as its HCl salt) to 150 mM Na₃PO₄ (I = 0.9) and 150 mM D₃PO₄ (ionic strength brought to I = 0.9 using NaCl) respectively. A pH probe was placed in the alkaline solution (5 mL) with stirring bar, and the pH meter output was read and noted. The pD value was obtained by adding 0.41 to the pH-meter value.²⁵ Approximately 0.7 mL was removed from the solution and placed in an NMR tube. A ¹H NMR spectrum was recorded. The NMR solution was returned to the pH-probed stirred vessel. The acidic solution was added dropwise to the pH-probed stirred solution until the pH-meter value (pD value) dropped by an amount not exceeding 0.25–0.50 units. The pH-meter value/pD value was again noted. Again, approximately 0.7 mL of the solution was transferred to an NMR tube and an NMR spectrum was recorded. The NMR solution was returned to the pH-probed stirred vessel. The procedure was repeated until such time as the pH meter value/pD value falls to well below (3 to 4 units) the expected pK_a value of the proline derivative under investigation. The NMR spectra obtained at the various pH meter/pD values was compiled and where possible the chemical shifts of all protons (in Hz) in all spectra were noted in a spreadsheet in which each row represented a spectrum taken at a particular pD value, and the columns represented chemical shifts of the specific protons. Using these data, the difference in chemical shifts (δ in Hz) of an appropriate pair of protons was calculated and plotted against the associated pD value. An appropriate pair of protons was deemed to be that where the associated chemical shifts could be determined accurately (that is, not obscured in any way within the pD range measured) and where the δ over the pD range was as large as possible (thus reducing the error). Using GraphPad Prism software, the plot was fitted with the best sigmoidal curve. The pD value at the inflection point of the fitted curve represents the pK_a value of the proline derivative. The value was verified by plotting the δ of an alternative pair of protons against pD.

Determination of the Rate of Deuterium/Hydrogen Incorporation as a Function of pD/pH. Preparation of Buffers.—150 mM phosphate D₂O buffers of constant ionic strength (I = 0.9) of various pD values were prepared as follows. A pH-meter probe was

immersed in a 10-mL Falcon® tube containing 5 mL of a 150 mM D₂O solution of Na₃PO₄ ($I=0.9$). A 150 mM D₂O solution of D₃PO₄ ($I=0.9$, NaCl) was added dropwise until the desired pD value was reached (pD value = pH-meter value + 0.41). For the preparation of 150 mM imidazole D₂O buffers of constant ionic strength ($I=0.150$) of various pD values, the above procedure was followed using 150 mM D₂O solutions of imidazole (with 0.150 mM of NaCl) and imidazole DCl salt. For the preparation of 150 mM phosphate D₂O/H₂O (1:1) buffers of constant ionic strength ($I=0.9$) at various pH-meter reading values, the above procedure was followed using a 150 mM H₂O/D₂O (1:1) solution of Na₃PO₄ and a 150 mM H₂O/D₂O (1:1) solution of D₃PO₄ ($I=0.9$, NaCl).

¹H NMR Method for Determination of the Rate of Deuterium Incorporation.—A 150 mM D₂O solution of phosphate of the pD value under investigation (1 mL) was placed in a 5-mL vial. Cyclohexanone (20 μL, 0.193 mmol) was added, and the capped vial was vortexed for 10 s. A D₂O solution of the catalyst under investigation (an amount representing approximately 10 mol% (0.0193 mmol) with an added volume of no greater than 50 μL) was added, and the resulting mixture was vortexed for 10 s. A 0.7-mL aliquot of the homogeneous solution was immediately placed in an NMR tube, and the tube was inserted into the NMR probe. ¹H NMR spectra were recorded at constant intervals. Using Bruker software, the multizg function was employed with the number of scans (ns) was set to 4, and the number of dummy scans (ds) set to a value between 20 and 70 (depending upon the rate of reaction); between 10 and 50 consecutive acquisitions were recorded wherein the ds value represents the interval between acquisitions. The exact time between acquisitions was determined by examining the time interval between the storage of consecutive FID files. The resultant FID files were processed using MestReNova software. The number of moles of deuterium nuclei per liter of reaction solution incorporated into the α positions of cyclohexanone was calculated by subtracting the integration of the α protons from that of the β protons (the integration of the β protons corresponds to 0.736 M; 0.193 mmol of cyclohexanone in ~1.050 mL of solution represents 0.184 M, multiplied by 4 because there are 4 α and 4 β protons). In some samples, signals from the catalyst overlapped with the α protons of cyclohexanone; in those cases, the appropriate correction was made. The amount of deuterium incorporated (M) was plotted against the period of time between the start of the reaction, and the time of acquisition (s); the first acquisition was set at $t=0$ s. Spectra where 10% of possible deuterium incorporation was exceeded were discarded. The initial rates (M·s⁻¹) were determined by extracting the slope from the best line to fit the data (using GraphPad Prism software). For each catalyst the initial rate calculated at each pD value was plotted against pD.

Determination of Rate Laws.—For each catalyst, the rate-law exponent of each of the three reaction components (namely catalyst, ketone and buffer) was determined by measuring the rate of deuterium incorporation at various concentrations of the component under investigation whilst maintaining constant the concentration of the remaining components. The rates were measured using ¹H NMR spectroscopy according to the procedure outlined above. The log of the rate was then plotted against the log of the concentration of the component being varied; the slope of the resulting line represents the pertinent exponent. Because the mechanism and/or the identity of the turnover-rate-

determining transition state/intermediate could depend on the pD value of the solution, the exponents were usually determined at a pD value where catalysis was most efficient for the particular catalyst under investigation. The exponent of the catalyst and the ketone were determined at 0.15 M phosphate ($I = 0.9$). To obtain the exponent of the buffer, D₂O solutions of varying concentration of phosphate (0.05–0.5 M) of the same ionic strength ($I = 3.0$) and pD value were prepared. These solutions were prepared as follows: D₂O solutions of 0.5 M Na₃PO₄ ($I = 3.0$) and 0.5 M D₃PO₄ ($I = 3.0$, NaCl) were prepared. Through appropriate dilution of aliquots of these solutions with D₂O (3.0 M NaCl), solutions of Na₃PO₄ and D₃PO₄ of varying concentration of phosphate (0.05 to 0.5 M in intervals of 0.05 M) and constant ionic strength ($I = 3.0$) were prepared. Using a pH meter, the appropriate pairs of acidic and basic solutions were combined to obtain a solution of a particular concentration of phosphate at a particular pD value. The background rate (catalysis of exchange by aminocatalyst alone) was subtracted from the observed rate to obtain an exponent that was predominantly associated with iminium/enamine/phosphate catalysis by the proline derivative.

Investigation of Substrate Isotope Effects.—The rate of incorporation of hydrogen and deuterium into [D₀]cyclohexanone and [D₄]cyclohexanone, respectively, as catalyzed by the proline derivative under investigation, were determined in 1:1 mixtures of phosphate-buffered (150 mM, $I = 0.9$) D₂O and H₂O of a particular pH-meter reading. The use of a common reaction medium for the comparison of rates of the exchange reaction of [D₀]cyclohexanone and that of [D₄]cyclohexanone reduces errors and, more importantly, allows the isotope effects pertaining to species derived from the solvent, the buffer, and the substrate to be disentangled. The D₂O and H₂O buffers were prepared according to the method described above and then mixed in the required ratio (1:1; total volume: 1 mL). A D₂O/H₂O solution (1:1; total volume: 70 μL) of the catalyst (0.0193 mmol) was added to the mixture. [D₀]Cyclohexanone (0.193 mmol, 20 μL) was then added, and the mixture was shaken vigorously for 10 s to ensure homogeneity; at the same time, a stopwatch was started. For a period ranging from 1–2 h, at intervals ranging from 10–20 min, 100 μL of the mixture was removed and added to a vial containing 1.0 mL of CH₂Cl₂ and suspended sodium sulfate. The vial was sealed and shaken. The resulting solution of CH₂Cl₂ was decanted and passed through a short silica plug, which was prepared using a Pasteur pipette, cotton wool, silica gel, sand, and when prepared contained approximately 2–3 cm of silica gel. The filtrate was placed in a labelled vial suitable for GS/MS analysis. When the experiment was complete, the prepared vials, together with a vial containing a solution of fresh [D₀]cyclohexanone in CH₂Cl₂ as a standard, were analyzed using GS/MS. The above procedure was repeated using [D₄]cyclohexanone. For each vial, the peak corresponding to the mixture of cyclohexanone isotopes was integrated, and the relative amounts of each mass ion tabulated in an Excel spreadsheet. For the experiments using [D₀]cyclohexanone ($M = 98$), integrations corresponding to a species ($M = 97$) and its associated $M + n$ ions ($n = 1$ and 2), which were calculated assuming natural abundance, were subtracted. The resultant integration values associated with $M = 98$, $M = 99$, and $M = 100$ were assumed to represent the sum of the integrations associated with [D₀]cyclohexanone, [D₁]cyclohexanone, and [D₂]cyclohexanone of both natural and non-natural (derived from the reaction) abundance. The relative amounts of [D₁]cyclohexanone and [D₂]cyclohexanone, as derived from the

reaction, expressed as a percentage of the sum of the amounts corresponding to [D₀]-, [D₁]-, and [D₂]cyclohexanone, were determined by sequential subtraction. The relative amounts of [D₁]cyclohexanone and [D₂]cyclohexanone of non-natural abundance were added and converted into moles of deuterium incorporated, and the values were plotted against time (in seconds). A similar analysis was done for the incorporation of hydrogen into [D₄]cyclohexanone. The slopes of the resulting graphs were expressed as a ratio to determine k_H/k_D .

Supplementary Material

Refer to Web version on PubMed Central for supplementary material.

ACKNOWLEDGEMENTS

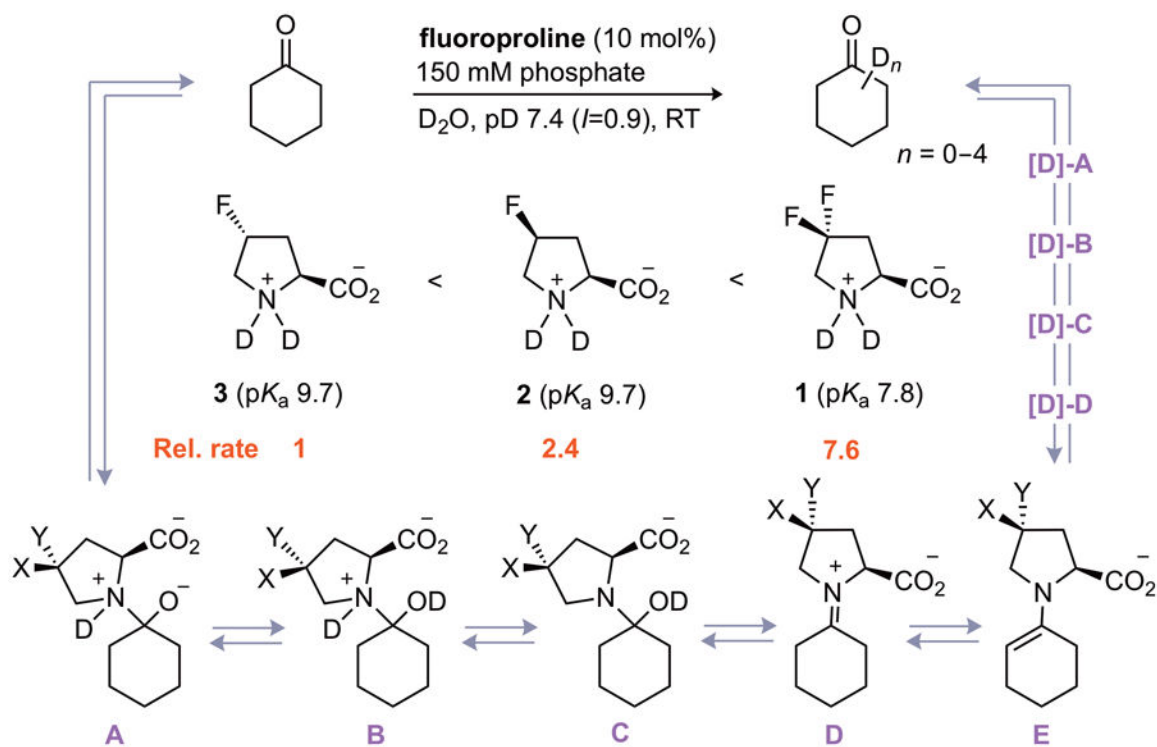
E.M. acknowledges support from the School of Chemistry, NUI-Galway. M.J.P. was supported by Molecular and Cellular Pharmacology Training Grant T32 GM008688 (NIH) and predoctoral fellowship 09PRE2260125 (American Heart Association). This work was supported by grants R01 AR044276 and R01 GM044783 (NIH). NMRFAM was supported by grant P41 GM103399 (NIH).

REFERENCES

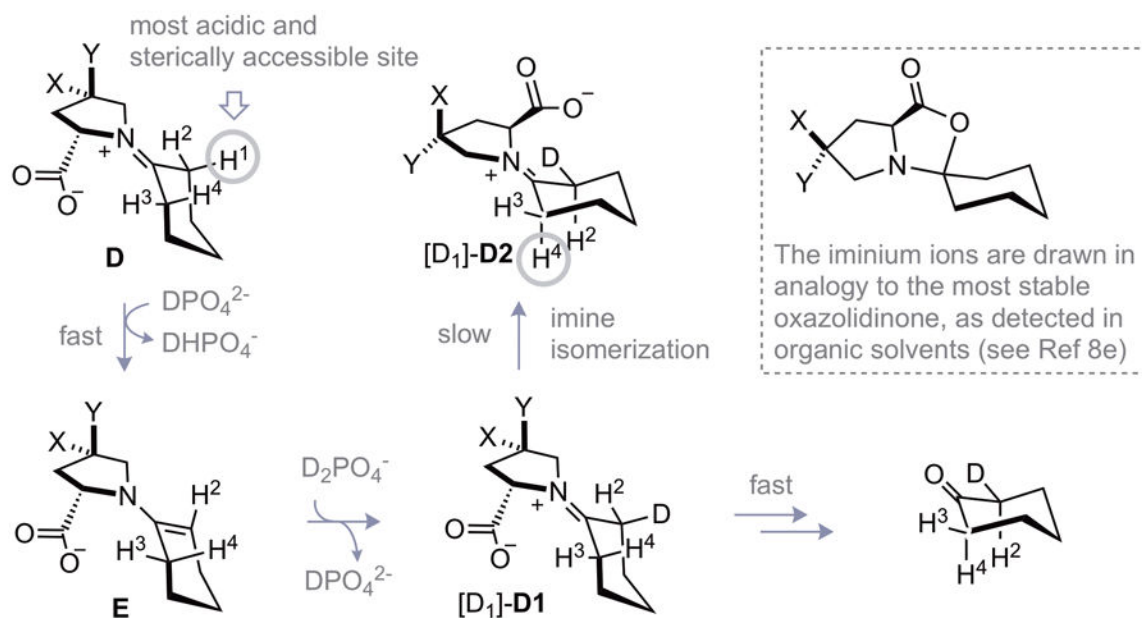
- (1) (a). Notz W; Tanaka F; Barbas CF III Enamine-Based Organocatalysis with Proline and Diamines: The Development of Direct Catalytic Asymmetric Aldol, Mannich, Michael, and Diels–Alder Reactions. *Acc. Chem. Res* 2004, 37, 548–557. (b) List B Enamine Catalysis Is a Powerful Strategy for the Catalytic Generation and Use of Carbanion Equivalents. *Acc. Chem. Res* 2005, 38, 548–557. (c) Berkessel A; Gröger H Asymmetric Organocatalysis, Wiley–VCH, Weinheim, 2005. (d) Enantioselective Organocatalysis: Reactions and Experimental Procedures, (Ed.: Dalako PI), Wiley–VCH, Weinheim, 2007. (e) Melchiorre P; Marigo M; Carlone A; Bartoli G Asymmetric Aminocatalysis—Gold Rush in Organic Chemistry. *Angew. Chem., Int. Ed* 2008, 47, 6138–6171. (f) Asymmetric Organocatalysis (Ed.: List B), *Top. Curr. Chem* Vol 291, Springer, Heidelberg and Berlin, 2009. (g) Pellissier H Recent Developments in Asymmetric Organocatalysis, Royal Society of Chemistry, Cambridge, 2010.
- (2) (a). For accounts on the origins of aminocatalysis, see: MacMillan DW The Advent and Development of Organocatalysis. *Nature*, 2008, 455, 304–308. [PubMed: 18800128] (b) List B Emil Knoevenagel and the Roots of Aminocatalysis. *Angew. Chem., Int. Ed* 2010, 49, 1730–1734. For a prominent early example of an asymmetric aminocatalytic reaction, see: (c) Eder U; Sauer G; Wiechert R New Type of Asymmetric Cyclization to Optically Active Steroid CD Partial Structures. *Angew. Chem., Int. Ed* 1971, 10, 496–497. (d) Hajos ZG; Parrish DR Asymmetric Synthesis of Bicyclic Intermediates of Natural Product Chemistry. *J. Org. Chem* 1974, 39, 1615–1621.
- (3) (a). List B Lerner RA Barbas CF III Proline-Catalyzed Direct Asymmetric Aldol Reactions. *J. Am. Chem. Soc* 2000, 122, 2395–2396. (b) Ahrendt KA; Borths CJ; MacMillan DWC New Strategies for Organic Catalysis: The First Highly Enantioselective Organocatalytic Diels–Alder Reaction. *J. Am. Chem. Soc* 2000, 122, 4243–4244. For a review on early work reported at the turn of the millennium, see: (c) Jarvo ER; Miller SJ Amino Acids and Peptides as Asymmetric Organocatalysts. *Tetrahedron* 2002, 58, 2481–2495.
- (4). For a remarkable example of low aminocatalyst loading, see: Wiesner M; Upert G; Angelici G; Wennemers H Enamine Catalysis with Low Catalyst Loadings - High Efficiency via Kinetic Studies. *J. Am. Chem. Soc* 2010, 132, 6–7. [PubMed: 19791790]
- (5). Raj M; Singh VK Organocatalytic Reactions in Water. *Chem. Commun* 2009, 6687–6703.
- (6). Spears RJ; Brabham RL; Budhadev D; Keenan T; McKenna S; Walton J; Brannigan JA; Brzozowski AM; Wilkinson AJ; Plevin M; Fascione MA Site-Selective C–C Modification of Proteins at Neutral pH Using Organocatalyst-Mediated Cross Aldol Ligations. *Chem. Sci* 2018, 9, 5585–5593. [PubMed: 30061990]

- (7) (a). Stepankova V; Bidmanova S; Koudelakova T; Prokop Z; Chaloupkova R; Damborsky J Strategies for Stabilization of Enzymes in Organic Solvents. *ACS Catal* 2013, 3, 2823–2836. (b)Carrea G; Riva S Properties and Synthetic Applications of Enzymes in Organic Solvents. *Angew. Chem., Int. Ed* 2000, 39, 2226–2254.
- (8) (a). Renzi P; Hioe J; Gschwind RM Enamine/Dienamine and Brønsted Acid Catalysis: Elusive Intermediates, Reaction Mechanisms, and Stereinduction Modes Based on in Situ NMR Spectroscopy and Computational Studies. *Acc. Chem. Res* 2017, 50, 2936–2948. [PubMed: 29172479] (b)Burés J; Armstrong A; Blackmond DG Explaining Anomalies in Enamine Catalysis: “Downstream Species” as a New Paradigm for Stereocontrol. *Acc. Chem. Res* 2016, 49, 214–222. [PubMed: 26830669] (c)Nielsen M; Worgull D; Zweifel T; Gschwind B; Bertelsen S; Jørgensen KA Mechanisms in Aminocatalysis. *Chem. Commun* 2011, 47, 632–649. (d)Ha-Yeon Cheong P; Legault CY; Um JM; Celebi-Olcum N; Houk KN Quantum Mechanical Investigations of Organocatalysis: Mechanisms, Reactivities, and Selectivities. *Chem. Rev* 2011, 111, 5042–5137. [PubMed: 21707120] (e)Seebach D; Beck AK; Badine DM; Limbach M; Eschenmoser A; Treasurywala AM; Hobi R; Prikoszovich W; Linder B Are Oxazolidinones Really Unproductive, Parasitic Species in Proline Catalysis? – Thoughts and Experiments Pointing to an Alternative View. *Helv. Chim. Acta* 2007, 90, 425–471.
- (9) (a). Hughes DL Asymmetric Organocatalysis in Drug Development—Highlights of Recent Patent Literature. *Org. Process Res. Dev* 2018, 22, 574–584. (b)Bulger PG in *Comprehensive Chirality*, Vol. 9 (Eds.: Carreira EM; Yamamoto H), Elsevier, Amsterdam, 2012; Chapter 10, pp 228–252. (c)Xu F in *Sustainable Catalysis: Challenges and Practices for the Pharmaceutical and Fine Chemical Industries*, (Eds.: Dunn P; Krische MJ; Williams MT), John Wiley and Sons, Hoboken, NJ, 2013, pp 317–337.
- (10). Newberry RW; Raines RT 4-Fluoroprolines: Conformational Analysis and Effects on the Stability and Folding of Peptides and Proteins. *Top. Heterocycl. Chem* 2017, 48, 1–26. [PubMed: 28690684]
- (11) (a). Volkova NV; Shilov EA; Yasnikov AA Catalytic Action of Amino Acids and Amines in Organic Reactions of Carbonyl Compounds. XVI. Kinetics and Mechanism of the Iodination of Acetol-Phosphate in the Presence of Ethylenediamine. *Ukr. Khim. Zh* 1965, 31, 56 For a modern application of this exchange reaction, see: (b)Zhan M; Zhang T; Huang H; Xie Y; Chen Y A Simple Method for α -Position Deuterated Carbonyl Compounds with Pyrrolidine as Catalyst. *J. Label. Compd. Radiopharm* 2014, 57, 533–539.
- (12). The pKa values were measured in D₂O (150 mM phosphate, I = 0.9) by using ¹H NMR spectroscopy; see the Experimental Section and Supporting Information for details.
- (13) (a). Chandler CL; List B Catalytic Asymmetric Transannular Aldolizations: Total Synthesis of (+)-Hirsutene. *J. Am. Chem. Soc* 2008, 130, 6737–6739. [PubMed: 18454521] (b)Yap DQJ; Cheerlavancha R; Lowe R; Wang S; Hunter L Investigation of cis- and trans-4-Fluoroprolines as Enantioselective Catalysts in a Variety of Organic Transformations. *Aust. J. Chem* 2015, 68, 44–49. For reviews on recent developments on the use of C–F bonds in catalyst design, see: (c)Hunter L The C–F bond as a Conformational Tool in Organic and Biological Chemistry. *Beilstein J. Org. Chem* 2010, 6, 38. [PubMed: 20502650] (d)Zimmer LE; Sparr C; Gilmour R Fluorine Conformational Effects in Organocatalysis: An Emerging Strategy for Molecular Design. *Angew. Chem., Int. Ed* 2011, 50, 11860–11871.
- (14) (a). Eberhardt ES; Panasik N Jr.; Raines RT Inductive Effects on the Energetics of Prolyl Peptide Bond Isomerization: Implications for Collagen Folding and Stability. *J. Am. Chem. Soc* 1996, 118, 12261–12266. For a tutorial review on C–F bonds, see: [PubMed: 21451735] (b)O’Hagan D Understanding Organofluorine Chemistry. An Introduction to the C–F Bond. *Chem. Soc. Rev* 2008, 37, 308–319. [PubMed: 18197347]
- (15). Hine J Bifunctional Catalysis of α -Hydrogen Exchange of Aldehydes and Ketones. *Acc. Chem. Res* 1978, 11, 1–7.
- (16) (a). Gold V Protolytic Processes in H₂O–D₂O Mixtures. *Adv. Phys. Org. Chem* 1969, 7, 259–331. (b)Kresge AJ; Tang YC Hydrogen Isotope Fractionation Between Water and Aqueous Mono- and Dihydrogen Phosphate Ions. *J. Phys. Chem* 1979, 83, 2156–2159.
- (17). Jones JM; Bender ML Secondary Deuterium Isotope Effects in the Addition Equilibria of Ketones. *J. Am. Chem. Soc* 1960, 82, 6322–6326.

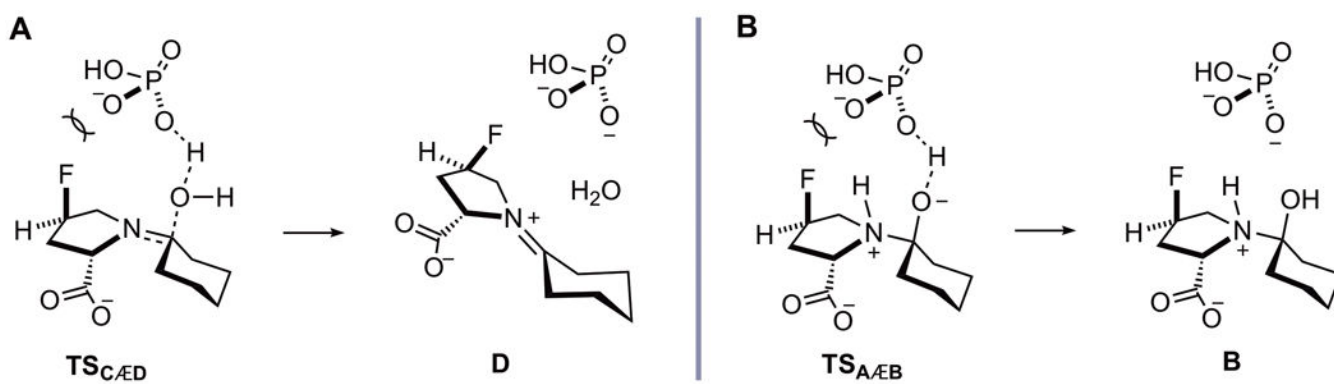
- (18). Bock DA; Lehmann CW; List B Crystal Structures of Proline-Derived Enamines. Proc. Natl. Acad. Sci. USA 2010, 107, 20636–20641. [PubMed: 21068369]
- (19). Hine J; Li W-S Catalysis of α -Hydrogen Exchange XIX. Bifunctional Catalysis of the Dedeuteration of Acetone-d₆ by Conformationally Constrained Derivatives of N,N-Dimethyl-1,3-propanediamine. J. Am. Chem. Soc 1976, 98, 3287–3294.
- (20). Hine J; Via FA; Gotkis JK; Craig JC Jr. Kinetics of the Formation of N-Isobutylidenemethylamine from Isobutyraldehyde and Methylamine in Aqueous Solution. J. Am. Chem. Soc 1970, 92, 5186–5193.
- (21). Keeffe JR; Jencks WP Large Inverse Solvent Isotope Effects: A Simple Test for the E1cB Mechanism. J. Am. Chem. Soc 1981, 103, 2457–2459.
- (22). Hollenstein M Synthesis of Deoxynucleoside Triphosphates that Include Proline, Urea, or Sulfonamide Groups and Their Polymerase Incorporation into DNA. Chem. Eur. J 2012, 18, 13320–13330. [PubMed: 22996052]
- (23) (a). Haberfield P; Pessin J Proximate Charge Effects. 3. Enthalpies of Solvent Transfer of Reactants and Transition States in the Saponification of Acetylcholine. J. Am. Chem. Soc 1983, 105, 526–528. (b) Schnieder H-J; Schneider U Host–Guest Chemistry. Part 9. Inhibition of Choline Acetate Hydrolysis in the Presence of a Macrocyclic Polyphenolate. J. Org. Chem 1987, 52, 1613–1615.
- (24). Marusawa H; Setoi H; Sawada A; Kuroda A; Seki J; Motoyama Y; Tanaka H Synthesis and Biological Activity of 1-Phenylsulfonyl-4-Phenylsulfonylaminopyrrolidine Derivatives as Thromboxane A₂ Receptor Antagonists. Bioorg. Med. Chem 2002, 1399–1415. [PubMed: 11886803]
- (25). Covington AK; Paabo M; Robinson RA; Bates RG Use of the Glass Electrode in Deuterium Oxide and the Relation Between the Standardized pD (paD) Scale and the Operational pH in Heavy Water. Anal. Chem 1968, 40, 700–706.

**Scheme 1.**

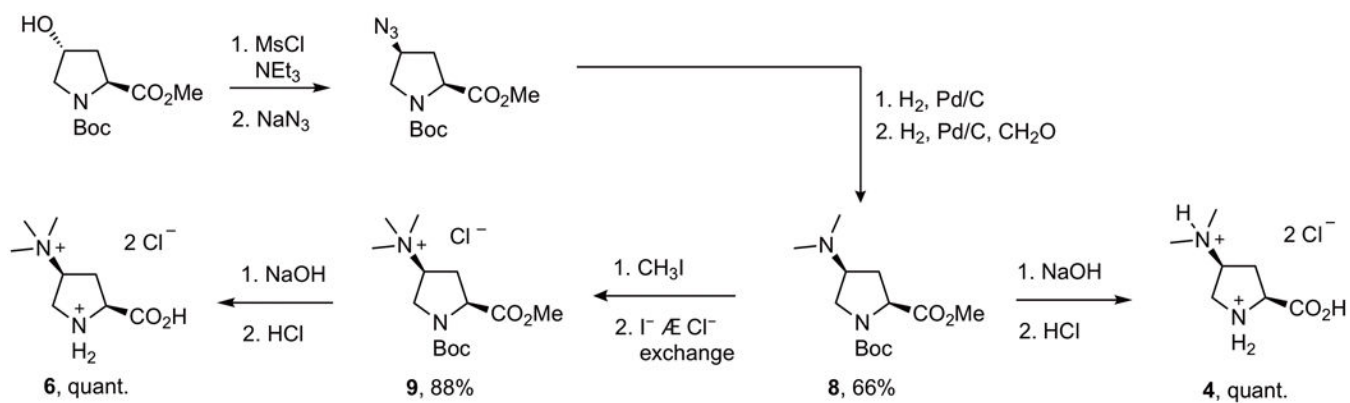
Relative catalytic activity of fluoroprolines at pD 7.4 and putative intermediates in the isotope exchange reaction of cyclohexanone.

**Scheme 2.**

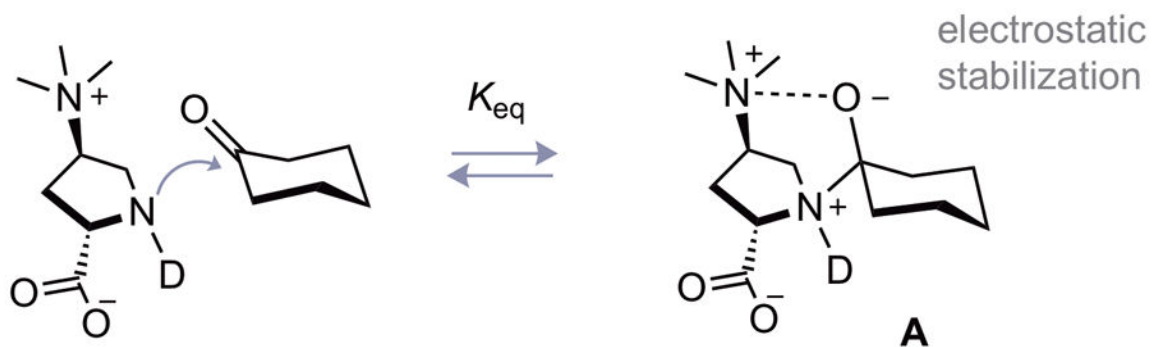
Proposed selective abstraction of the axial hydrogen atom distal and anti to the carboxylate substituent of the iminium intermediate.



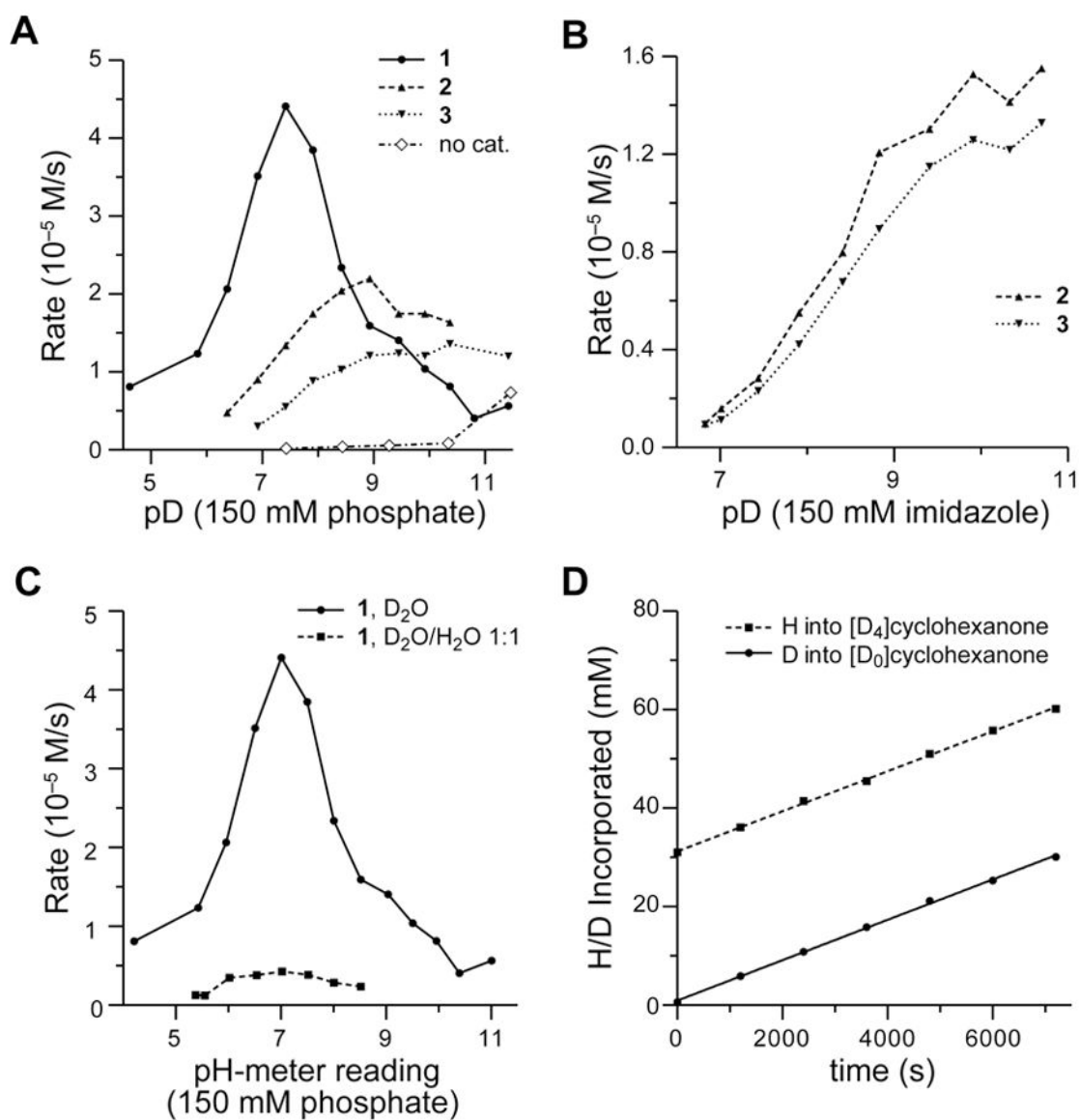
Scheme 3.
Destabilizing interactions in phosphate-mediated transformation of *trans*-4-fluoroproline intermediates in the hydrogen–deuterium exchange reaction of cyclohexanone



Scheme 4.
 Synthesis of *cis* 4-aminoproline **4** and **6**.

**Scheme 5.**

Proposed electrostatic interaction between the α -quaternary oxy-anion group and the ammonium group on the 4-position of the pyrrolidine ring in carbinoxyammonium **A** derived from either **5** or **7**.

**Figure 1.**

(A) pD–rate profiles of exchange reactions catalyzed by **1**–**3** in phosphate-buffered D_2O ($I=0.9$); (B) pD–rate profiles of exchange reactions catalyzed by **2** and **3** in imidazole-buffered D_2O ($I=0.15$); (C) pD–rate profiles of the exchange reaction catalyzed by **1** in D_2O/H_2O (1:1, $I=0.9$); (D) Rate of exchange reactions of $[D_0]$ - and $[D_4]$ cyclohexanone, catalyzed by **1** in D_2O/H_2O (1:1, pH-meter reading 7.2, $I=0.9$).

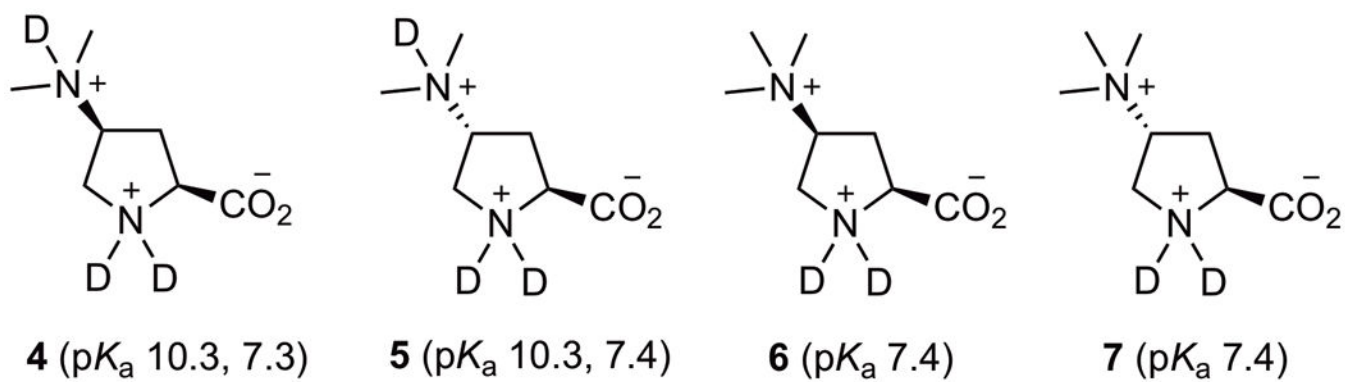
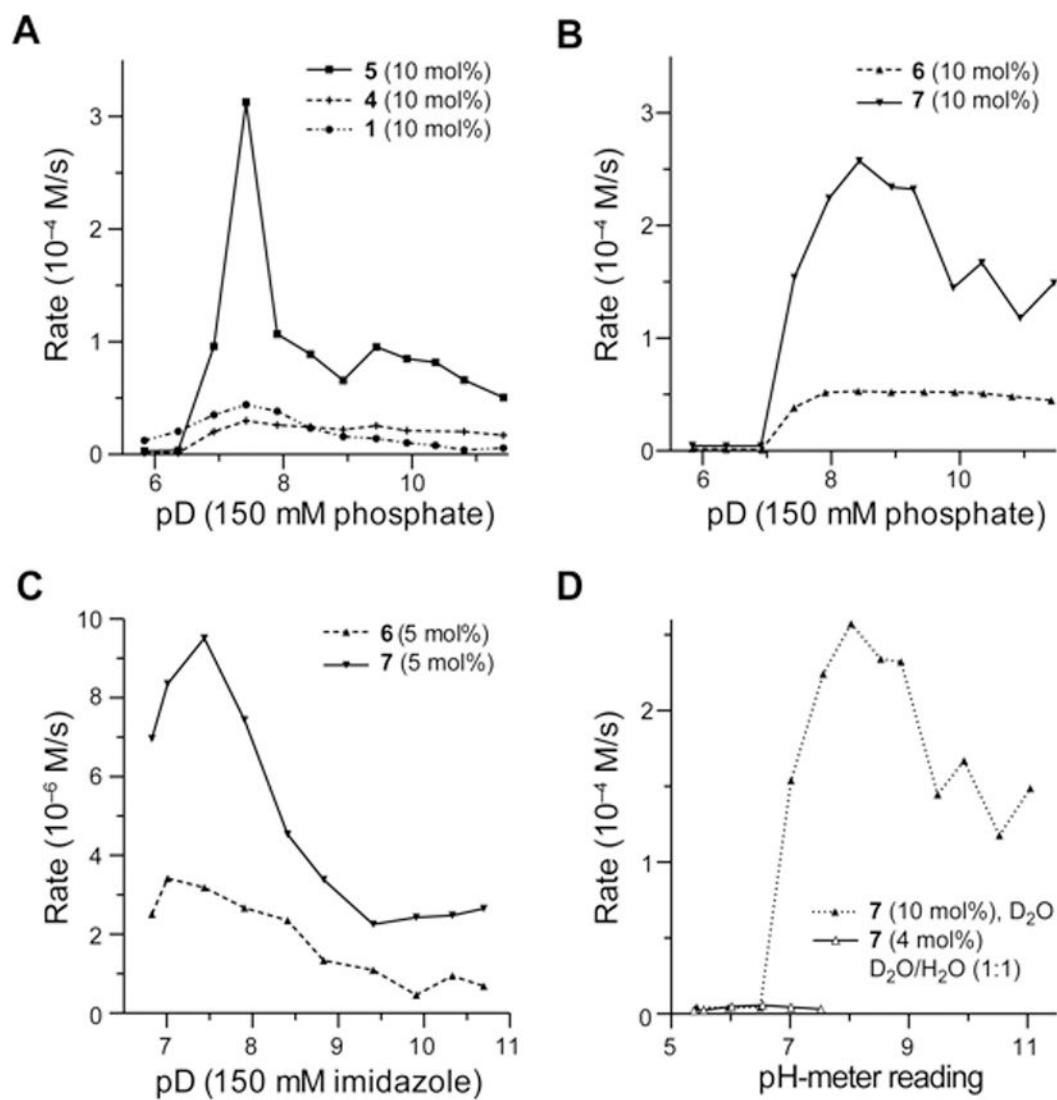
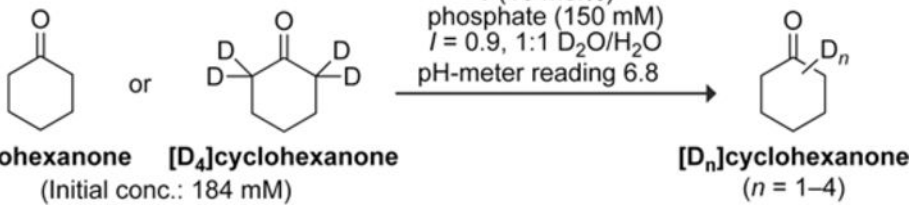


Figure 2.
Structures of aminoprolines 4–7.

**Figure 3.**

- (A) pD–rate profiles of reactions catalyzed by **4** and **5** in phosphate-buffered D_2O ($I = 0.9$).
 (B) pD–rate profiles of reactions catalyzed by **6** and **7** in phosphate-buffered D_2O ($I = 0.9$);
 (C) pD–rate profiles of reactions catalyzed by **6** and **7** in imidazole-buffered D_2O ($I = 0.15$);
 (D) pD–rate profiles of reactions catalyzed by **7** in D_2O/H_2O (1:1; $I = 0.9$).

Table 1Substrate Isotope Effects Determined in H₂O/D₂O (1:1).



pH meter reading	[H ₂ O]/[D ₂ O]	[DA]/[HA]	$k_{\text{H} \rightarrow \text{D}}/k_{\text{D} \rightarrow \text{H}}$	$k_{\text{H}}/k_{\text{D}}$
6.0	1.0	1.03	1.02	0.99
8.0	1.0	0.91	0.92	1.01